


Deterministic Generation of Large Fock States

M. Uria¹, P. Solano^{2,3} and C. Hermann-Avigliano^{1,*}

¹*Departamento de Física and Millennium Institute for Research in Optics (MIRO), Facultad de Ciencias Físicas y Matemáticas, Universidad de Chile, Santiago 8370448, Chile*

²*Department of Physics, MIT-Harvard Center for Ultracold Atoms, and Research Laboratory of Electronics, Massachusetts Institute of Technology, Cambridge, Massachusetts 02139, USA*

³*Departamento de Física, Facultad de Ciencias Físicas y Matemáticas, Universidad de Concepción, Concepción 160-C, Chile*

 (Received 10 March 2020; accepted 4 August 2020; published 28 August 2020)

We present a protocol to deterministically prepare the electromagnetic field in a large photon number state. The field starts in a coherent state and, through resonant interaction with one or few two-level systems, it evolves into a coherently displaced Fock state without any postselection. We show the feasibility of the scheme under realistic parameters. The presented method opens a door to reach Fock states, with $n \sim 100$ and optimal fidelities above 70%, blurring the line between macroscopic and quantum states of the field.

DOI: [10.1103/PhysRevLett.125.093603](https://doi.org/10.1103/PhysRevLett.125.093603)

Introduction.—Fock states are quantum states of the electromagnetic field with a well defined number of excitations. Such states are of significant theoretical and experimental interest, with applications ranging from protocols for quantum information to quantum metrology [1], where the quantum properties of the field allow for sensitivities greater than the achievable with classical light [2]. All these applications benefit from a fast and efficient generation of Fock states with a large number of photons, a long standing goal for the quantum optics community [3–11].

There are several theoretical proposals and experimental implementations for generating Fock states across different platforms, such as acoustic waves in resonators [8], photonic wave guides [12–14] and superconducting circuits [15–18]. In the context of cavity quantum electrodynamics (CQED), Fock states can be generated by injecting one quanta at a time into a cavity field [7,19], by resonantly interacting a jet of atoms passing through the cavity leaving the field in a upper-bounded steady Fock state [20,21], or by realizing quantum nondemolition measurements progressively projecting the field into a Fock state [22–26].

State of the art experiments generate Fock states with either low photon number ($n \sim 7-15$) [25,27,28], low fidelity at large photon numbers ($F > 80\%$ for $n \leq 4$ and $F < 50\%$ for $n \geq 4$) [23], or low probability of success after long convergence times ($\sim 80\%$ after ~ 20 ms) [24], evidencing the difficulty of the problem and the efforts made to generate arbitrarily large number states.

In this Letter we propose a protocol to deterministically generate large photon number states with significantly large fidelities, depicted in Fig. 1 with a CQED example. We consider a two-level atom that resonantly interacts with a coherent state. We show that, for particular interaction

times, the field evolves into a Fock-like state, slightly displaced in phase space. In the absence of decoherence, this protocol allows for fidelities above 70% for $n \sim 100$. This process can be sped up by simultaneously interacting two or more entangled atoms with the field. Under realistic losses, this scheme could generate Fock states as large as $n = 50$ with a fidelity of 58% in a CQED system [29] and a Fock states with $n = 100$ with a fidelity above 60% considering the state of the art in circuit QED [30–32]. Finally, we discuss the main characteristics and results of

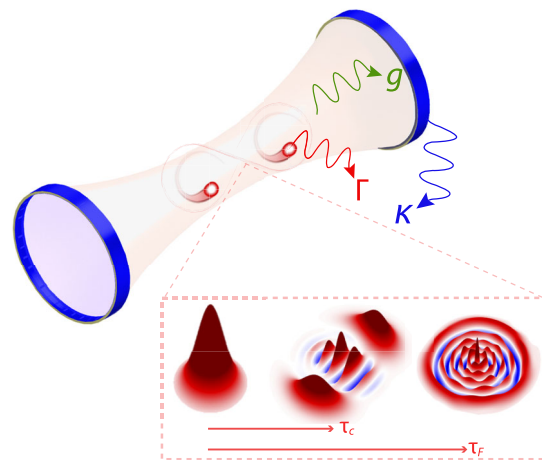


FIG. 1. Schematic of the proposal. One or two (entangled) two-level atoms interact with a coherent state trapped in a cavity. The field, represented here by its Wigner function, evolves from a coherent state to a macroscopic superposition (after an interaction time τ_C) and then into a Fock-like state (after an interaction time τ_F). The timescale of the evolution is set by coupling strength g . The final state of the field approaches to a Fock-like state, despite the cavity and atomic decay, given by the rates κ and Γ .

the protocol, and give an outlook of some open questions and future possibilities.

Theoretical model.—The interaction of an atom with the electromagnetic field inside a cavity is well described by the Jaynes-Cummings Hamiltonian [33]

$$\hat{H} = \frac{\hbar\omega_0}{2}\hat{\sigma}_z + \hbar\omega_c\hat{a}^\dagger\hat{a} + \hbar g(\hat{a}\hat{\sigma}_+ + \hat{a}^\dagger\hat{\sigma}_-), \quad (1)$$

where ω_0 and ω_c are the atomic and field frequencies, $g = \Omega_0/2$ is the coupling frequency, \hat{a} and \hat{a}^\dagger are the field operators, and $\hat{\sigma}_+$ and $\hat{\sigma}_-$ are the raising and lowering atomic operators. The evolution under resonant interaction ($\omega_c = \omega_0$) of the atom-field compound state ρ is determined by the master equation [1]

$$\begin{aligned} \hbar i \frac{d\rho(t)}{dt} &= [H_{\text{int}}, \rho(t)] \\ &- \frac{\kappa}{2}(n_{\text{th}} + 1)(\hat{a}^\dagger\hat{a}\rho(t) + \rho(t)\hat{a}^\dagger\hat{a} - 2a\rho(t)a^\dagger) \\ &- \frac{\kappa}{2}n_{\text{th}}(a\hat{a}^\dagger\rho(t) + \rho(t)a\hat{a}^\dagger - 2a^\dagger\rho(t)a) \\ &- \frac{\Gamma}{2}(n_{\text{th}} + 1)(\hat{\sigma}_+\hat{\sigma}_-\rho(t) + \rho(t)\hat{\sigma}_+\hat{\sigma}_- - 2\hat{\sigma}_-\rho(t)\hat{\sigma}_+) \\ &- \frac{\Gamma}{2}n_{\text{th}}(\hat{\sigma}_-\hat{\sigma}_+\rho(t) + \rho(t)\hat{\sigma}_-\hat{\sigma}_+ - 2\hat{\sigma}_+\rho(t)\hat{\sigma}_-), \end{aligned} \quad (2)$$

where $\hat{H}_{\text{int}} = \hbar g(\hat{a}\hat{\sigma}_+ + \hat{a}^\dagger\hat{\sigma}_-)$ is the Hamiltonian in the interaction representation, κ and Γ are the cavity and the atomic decay rates, respectively, and n_{th} is the average number of thermal photons.

We assume that the field is initialized in a coherent state of amplitude α and the state of the system is initially separable, meaning $\rho(0) = |\psi(0)\rangle\langle\psi(0)|$ with $|\psi(0)\rangle = |\phi_{\text{at}}\rangle|\alpha\rangle$.

The compound state initially factorizable, generally evolves into an entangled state. For a particular evolution time $\tau_C = 2\pi\sqrt{\bar{n}}/\Omega_0$, with $\bar{n} = |\alpha|^2$ being the average number of photons, the atom and the field get disentangled again and the field is found in a catlike state (see Fig. 1) [34,35]. Previous works have studied this system within such a time regime [36,37], nonetheless the exact evolution of the field at longer times has remain unexplored.

If we let the system interact for longer times we see that the Wigner function of the field temporarily evolves into a distribution that, at specific times $t = \tau_F$, resembles that of a Fock state [38] (see Fig. 1), but slightly displaced in phase space [39]. At $t = \tau_F$, the field and the atom become almost disentangled again, producing a field state that is nearly pure (purity $\approx 80\%$) [38]. By controlling the interaction time and injecting the proper field amplitude and phase to correct for the remnant coherent displacement, one can deterministically obtain a target Fock state.

The more commonly used figure of merit to quantify how close is the generated state $\rho_f(t) = \text{Tr}_{\text{at}}[\rho(t)]$ to an ideal Fock state with n photons (ρ_n) is the fidelity $F(\rho_f(t), \rho_n) = [\text{Tr}(\sqrt{\sqrt{\rho_n}\rho_f(t)\sqrt{\rho_n}})]^2$ [40]. Since the fidelity is not a proper metric, we characterize how similar both states are by calculating the function $1 - \delta(\rho_f(t), \rho_n)$, where $\delta(\rho_f(t), \rho_n) = \frac{1}{2}\text{Tr}(|\rho_f(t) - \rho_n|)$ is the trace distance [41]. Although we use one minus the distance trace for our calculations, we present our results in terms of the fidelity to provide a common-ground comparison with previous works.

We numerically calculate the evolution of the field state $\rho_f(t)$ under Eq. (2) and search for an optimum time $t = \tau_F$ that maximizes the value of $1 - \delta(\rho_f(t), \rho_n)$ for a target Fock state ρ_n . Because the field state evolves to something close to a Fock state but with a small displacement $D(\beta) (= \text{Exp}[\beta a^\dagger - \beta^* a])$, we applied a coherent displacement $-\beta$ after the field interacted with the atom [18,23,42,43]. We perform a numerical evaluation of the function $1 - \delta(\rho_f(t, \beta), \rho_n)$ and optimize it over two parameters, namely t and β , obtaining the optimal interaction time τ_F and its corresponding optimum coherent displacement β_F .

Results.—We first consider the case of a single atom initially in the excited state interacting with a resonant coherent field in the absence of any decoherence mechanism. Figure 2(a) shows, on the left axis, the maximum achievable $1 - \delta(\rho_f(t, \beta), \rho_n)$ between the obtained field (displaced by the proper β in each case) and a Fock state with n photons as a function n . The calculation is repeated for different initial coherent states with average photon number $|\alpha|^2 = \bar{n}$. We observe that the optimum generation of a Fock state happens at $n = \bar{n}$, meaning that the process benefits from keeping the same average number of excitations in the field. (An example of the energy conservation throughout the full evolution of the system is presented in the Supplemental Material [38].) For those cases, the fidelity can be higher than 75% for $n \leq 50$ as shown in the right axis of Fig. 2(a). Notice that the points plotted for the fidelity (with $n = \bar{n}$) correspond to the peaks of distributions like those shown in the $1 - \delta$ plots as a function of n for a fix \bar{n} . Figures 2(b) and 2(c) show the elements of the density matrix for the generated Fock-like states with $n = 10$ and $n = 60$, respectively. We observe a small remnant in the coherences that explains the obtained fidelities despite negligible population of adjacent number states.

Collective atomic effects increase the effective interaction strength, hence shortening the necessary interaction times to generate a target Fock state. Only a few initial atomic states lead to the formation of a Fock-like state. These are linear superpositions of the eigenstates $|\phi_{\lambda_i}\rangle$ of the collective atomic operator $\hat{S}_x^{(N)} = \sum_i^N \hat{\sigma}_x^{(i)}$, i.e.,

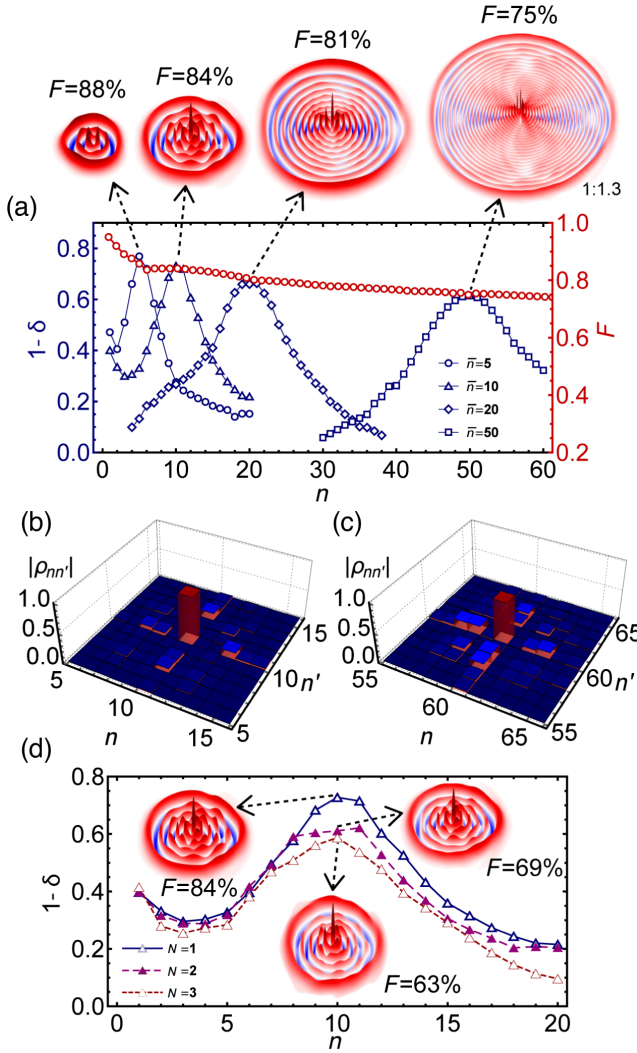


FIG. 2. (a) The left blue axis shows one minus the trace distance between the obtained state and $|n\rangle$ as a function of n , where a single two-level atom initially in $|e\rangle$ interacts with a coherent field α with different initial average number of photons $|\alpha|^2 = \bar{n} = \{5, 10, 20, 50\}$. The right red axis shows the obtained fidelity for $n = \bar{n}$ as a function of n . (b),(c) Density matrices of the generated Fock-like states with $n = 10$ and $n = 60$, respectively. (d) One minus the trace distance between the obtained state and $|n\rangle$ as a function of n for a field that starts in a coherent state $|\alpha|^2 = \bar{n} = 10$ and interacts with $N = \{1, 2, 3\}$ atoms. The insets on top of every curve represents the Wigner functions and fidelity of the obtained field state at $n = \bar{n}$.

$\hat{S}_x^{(N)}|\phi_{\lambda_i}\rangle = \lambda_i|\phi_{\lambda_i}\rangle$ with eigenvalues λ_i , where $\hat{\sigma}_x^{(i)}$ is the Pauli matrix operating on the i -th atom and N is the total number of atoms. In particular, the initial atomic states that lead to a Fock-like states are those of the form $|\phi_{\text{at}}\rangle = 1/\sqrt{2}(|\phi_{\lambda_1}\rangle + |\phi_{\lambda_2}\rangle)$, such that $\lambda_2 = -\lambda_1$. The formation of a Fock state speeds up by a factor of N when $\lambda_1 = \max\{\lambda_i\}$.

Figure 2(d) shows one minus the trace distance of the generated Fock state, as a function of n , for one,

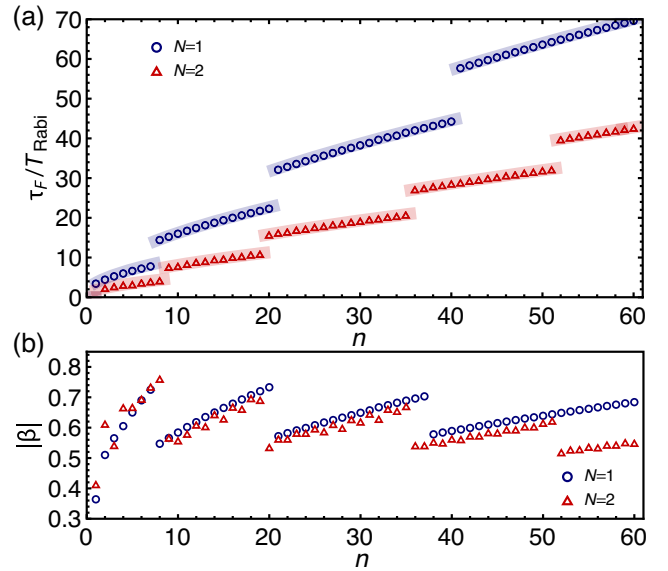


FIG. 3. (a) Optimum times τ_F to generate a Fock state $|n\rangle$ as a function of n , starting from a coherent state $|\alpha|^2 = \bar{n} = n$, for the case of a single atom in $|e_1\rangle$ (blue circles) and two entangled atoms in $(|e_1e_1\rangle + |g_1g_1\rangle)/\sqrt{2}$ (red triangles). The vertical axis is in units of resonant Rabi periods. (b) Displacements β_F for the states achieved in (a) as a function of n .

two, and three atoms. The initial atomic states are $|\phi_{\text{at}}\rangle = \{|e_1\rangle; (1/\sqrt{2})(|g_1g_2\rangle + |e_1e_2\rangle); \frac{1}{2}(|e_1e_2e_3\rangle + |e_1g_2g_3\rangle + |g_1e_2g_3\rangle + |g_1g_2e_3\rangle)\}$, respectively, where g_i and e_i represent the i th atom being in the ground or excited state, respectively. We see that increasing the number of atoms has a detrimental effect on the fidelity of the final Fock state, because the purity of the field gets compromised when a larger fraction of the total coherence of the system remains in the atomic subsystem [38]. Considering this, and the technical difficulties of realizing entangled states of many particles, we limit our analysis to the case of one and two atoms.

Figure 3(a) shows the optimum times τ_F in units of a single-atom or single-photon Rabi period as a function of the target number of photons n , for one and two atoms (same initial atomic states as before). The optimal evolution time τ_F follows even multiples of a $(\sqrt{n} + \sqrt{n+1})$ dependence [38], represented by segmented shaded lines. The multiple branches appear because the Fock-like state is periodically generated throughout the evolution of the system, but with slightly different fidelities. The maximization of the fidelity leads to what looks like jumps of τ_F between different branches [38]. Figure 3(b) shows the displacements β_F necessary to generate the Fock-like state with the largest fidelity as a function of n . In our case the displacement is always real, since we begin the interaction with a real α . If α were complex, then the appropriate displacement will have the same complex phase than α . The role of the coherent displacement $D(\beta_F)$ is to compensate for the energy difference between the initial or target state

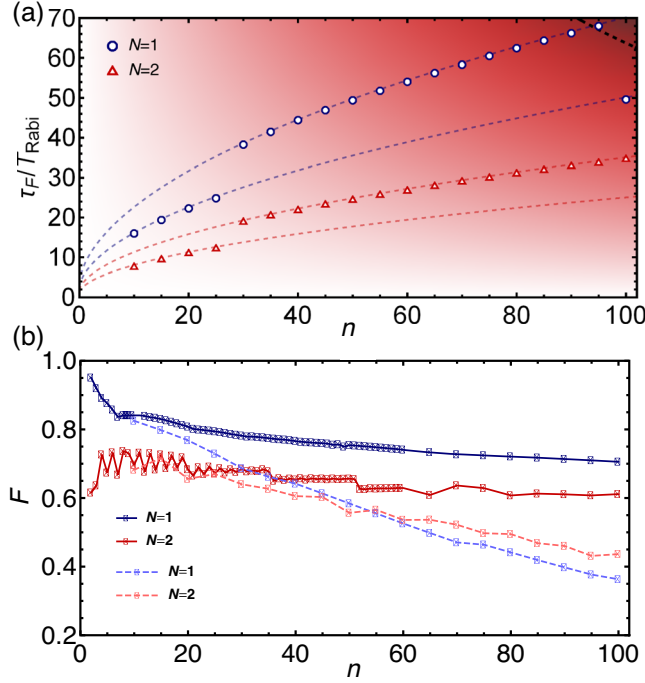


FIG. 4. (a) Optimum times τ_F to generate a Fock state $|n\rangle$ as a function of n , starting from a coherent state $|\alpha|^2 = \bar{n} = n$, for the one and two atom cases (see Fig. 2). The vertical axis is in units of resonant Rabi periods. Colored dashed line corresponds to the multiple branches of the solutions for both cases [38]. The black dashed line represents the decay time of a Fock state of n photons inside the cavity. (b) Fidelities for the states generated in (a) as a function of n . Continuous lines denote the ideal lossless system, and dashed lines denotes the system under realistic decoherence mechanisms in CQED.

and the final state of the field after energy exchange with the atoms [38].

Experimental feasibility in CQED.—We analyse our protocol for typical experimental parameters in CQED with Rydberg atoms [25] (see Fig. 1). We consider decoherence from cavity and atomic losses, and thermal photons (Eq. (2)) to be $\kappa = 1/T_c$, with $T_c = 130$ ms the cavity damping time, $\Gamma = 1/T_a$, with $T_a = 30$ ms the atomic lifetime, $n_{\text{th}} = 0.05$ (at 0.8 K) [44], and a vacuum Rabi frequency of $\Omega_0 = 2\pi \times 49$ kHz [1]. The atoms are sent through the cavity as a jet, and the interaction time is controlled by the atomic velocity. Figure 4(a) shows the optimum times τ_F as a function of n , for one and two atoms. The decay rate of a Fock states with n photons is κn [27], represented by the dashed line and a shaded area in Fig. 4(a). The extension of the scheme to larger photon number states or larger number of atoms is truncated by decoherence effects, and its exploration is limited by our computational capabilities. Figure 4(b) shows the maximum fidelity for one and two atoms as a function of the target Fock state, both in the ideal case and in the presence of decoherence. Notice that in the presence of decoherence one benefits of using two atoms for target Fock states

above $n = 50$. The obtained Fock-like states are robust against imperfections in both the evolution time τ_F and the coherent displacement β_F , where typical experimental errors produce negligible changes in the state fidelity [38,42].

State of the art of CQED experiments with Rydberg atoms can reach a maximum interaction time of 20 Rabi periods [45]. Although experimental improvements are being made on that regard, this presents an opportunity to study protocols for state preparation of a few entangled atoms to speed up the state generation process.

We observe that even for the simplest of the previously described cases, meaning a single excited atom interacting with a coherent state, it is possible to achieve larger fidelities by conditioning the field to a particular post-selected atomic state [1]. As a comparison, for an initial or target state $\bar{n} = n = 10$ and a single atom we obtain a fidelity of 92% upon measuring the atom in the excited state, compared with $F = 84\%$ in the unprojected case. A careful analysis of optimal projections on the atomic subsystem goes beyond the scope of this Letter, but it opens an opportunity to improve the presented scheme.

Our protocol for Fock states generation can be easily extended to other platforms. Circuit-QED systems are particularly interesting, since the interaction time between the artificial atom and the field is arbitrarily large. Considering parameters of state of the art circuit-QED experiments [30–32], it is possible to generate a Fock state near $n = 100$ with 60% fidelity with a single qubit, close to the performance of the protocol without decoherence.

Analysis and discussion.—We observe that the generation of Fock-like states requires two physical phenomena: nonlinearity and interference. Given that the effective Rabi frequency depends on the photon number as $\Omega = \Omega_0 \sqrt{n}$, the probability distribution of the coherent state will be distorted upon unitary evolution, resulting in the negativity of its Wigner function. This is a particular case of a nonlinear evolution generating a non-classical state [46]. On the other hand, when the interacting two-level system is in a superposition, the field evolves as such, allowing for interference effects among probability amplitudes of the field overlapping in phase space (see video in [38]). The nonlinear \hat{n} dependence and the ability to evolve the field in a superposition, generating Fock-like states, are not unique features of the Jaynes-Cummings model. For example, the effective interaction Hamiltonian $H_{\text{eff}} = g/2\sqrt{\hat{n}}\hat{S}_x^{(N)}$ [36,47] can also generate Fock-like states. While the nonlinearity-plus-interference picture explains the generation of highly nonclassical states, it does not answer why we can obtain Fock-like states in particular or why these have such large and robust fidelities. Nonetheless, it is not too surprising that the distribution of a field unitarily evolved to have a large phase uncertainty will resemble that of a Fock state. The most remarkable aspect of the presented protocol is the fact that a macroscopically intense classical

field can express its truly granular (quantum) nature upon interaction with a quantum two-level system.

The presented scheme could be implemented across different QED platforms. Its limiting factor is the shortest time scale for the decoherence. Since the system needs to undergo several Rabi cycles before the fields ends in a Fock-like state, we suspect that the necessary condition to succeed is that of strong coupling, where $g \gg n\kappa, \Gamma$.

Conclusions.—We have presented a protocol to deterministically generate large photon number state within QED systems. The field starts in a coherent state and evolves to a Fock-like state upon resonant interaction with a two-level system, without need of a postselective procedure. The intrinsic nonlinear evolution of the field plus interference effects in the photon number probability amplitudes generate a state of the field that is well described by a Fock state coherently displaced in phase space. After correcting for such displacement, we obtain a Fock-like state with optimal fidelities as large as 71% for $n = 100$. We show how this process can be sped up aided by a second two-level system, but compromising the fidelity of the final state. The scheme is shown to be feasible for current state-of-the-art experiments. Although our analysis is mainly focused on a CQED system, it can be extended to other QED platforms. We expect that the implementation of the presented protocol will have a significant impact on quantum metrology applications.

We thank Vlado Vuletić for helpful discussions at the genesis of this project and Jean-Michel Raimond and Bruno Peaudecerf for their useful comments and suggestions. The authors acknowledge J. Rojas for her help on figures design. This work was supported in part by FONDECYT Grant No. 11190078, CONICYT-PAI Grants No. 77190033 and No. 77180003, and Programa ICM Millennium Institute for Research in Optics (MIRO). All numerical calculations were performed with Julia Programming Language and libraries within.

*Corresponding author.
carla.hermann@uchile.cl

- [1] S. Haroche and J. M. Raimond, *Exploring the Quantum: Atoms, Cavities, and Photons* (Oxford University Press, Oxford, 2013), <https://dx.doi.org/10.1093/acprof:oso/9780198509141.001.0001>.
- [2] V. Giovannetti, S. Lloyd, and L. Maccone, *Nat. Photonics* **5**, 222 (2011).
- [3] B. T. H. Varcoe, S. Brattke, M. Weidinger, and H. Walther, *Nature (London)* **403**, 743 (2000).
- [4] S. Brattke, B. T. H. Varcoe, and H. Walther, *Phys. Rev. Lett.* **86**, 3534 (2001).
- [5] P. Bertet, S. Osnaghi, P. Milman, A. Auffeves, P. Maioli, M. Brune, J. M. Raimond, and S. Haroche, *Phys. Rev. Lett.* **88**, 143601 (2002).
- [6] E. Waks, E. Diamanti, and Y. Yamamoto, *New J. Phys.* **8**, 4 (2006).
- [7] M. Hofheinz, E. M. Weig, M. Ansmann, R. C. Bialczak, E. Lucero, M. Neeley, A. D. O'Connell, H. Wang, J. M. Martinis, and A. N. Cleland, *Nature (London)* **454**, 310 (2008).
- [8] Y. Chu, P. Kharel, T. Yoon, L. Frunzio, P. T. Rakich, and R. J. Schoelkopf, *Nature (London)* **563**, 666 (2018).
- [9] J. Tiedau, T. J. Bartley, G. Harder, A. E. Lita, S. W. Nam, T. Gerrits, and C. Silberhorn, *Phys. Rev. A* **100**, 041802(R) (2019).
- [10] R. Yanagimoto, E. Ng, T. Onodera, and H. Mabuchi, *Phys. Rev. A* **100**, 033822 (2019).
- [11] F. Dell'Anno, S. De Siena, and F. Illuminati, *Phys. Rep.* **428**, 53 (2006).
- [12] A. González-Tudela, V. Paulisch, D. E. Chang, H. J. Kimble, and J. I. Cirac, *Phys. Rev. Lett.* **115**, 163603 (2015).
- [13] A. González-Tudela, V. Paulisch, H. J. Kimble, and J. I. Cirac, *Phys. Rev. Lett.* **118**, 213601 (2017).
- [14] M. Perarnau-Llobet, A. González-Tudela, and J. I. Cirac, *Quantum Sci. Technol.* **5**, 025003 (2020).
- [15] P. J. Leek, M. Baur, J. M. Fink, R. Bianchetti, L. Steffen, S. Filipp, and A. Wallraff, *Phys. Rev. Lett.* **104**, 100504 (2010).
- [16] S. P. Premaratne, F. C. Wellstood, and B. S. Palmer, *Nat. Commun.* **8**, 14148 (2017).
- [17] X. Gu, A. F. Kockum, A. Miranowicz, Y.-x. Liu, and F. Nori, *Phys. Rep.* **718**, 1 (2017).
- [18] M. Hofheinz, H. Wang, M. Ansmann, R. C. Bialczak, E. Lucero, M. Neeley, A. O'Connell, D. Sank, J. Wenner, J. M. Martinis *et al.*, *Nature (London)* **459**, 546 (2009).
- [19] K. Vogel, V. M. Akulin, and W. P. Schleich, *Phys. Rev. Lett.* **71**, 1816 (1993).
- [20] P. Meystre, G. Rempe, and H. Walther, *Opt. Lett.* **13**, 1078 (1988).
- [21] M. Weidinger, B. T. H. Varcoe, R. Heerlein, and H. Walther, *Phys. Rev. Lett.* **82**, 3795 (1999).
- [22] C. Guerlin, J. Bernu, S. Deléglise, C. Sayrin, S. Gleyzes, S. Kuhr, M. Brune, J.-M. Raimond, and S. Haroche, *Nature (London)* **448**, 889 (2007).
- [23] S. Deléglise, I. Dotsenko, C. Sayrin, J. Bernu, M. Brune, J.-M. Raimond, and S. Haroche, *Nature (London)* **455**, 510 (2008).
- [24] C. Sayrin, I. Dotsenko, X. Zhou, B. Peaudecerf, T. Rybarczyk, S. Gleyzes, P. Rouchon, M. Mirrahimi, H. Amini, M. Brune, J.-M. Raimond, and S. Haroche, *Nature (London)* **477**, 73 (2011).
- [25] X. Zhou, I. Dotsenko, B. Peaudecerf, T. Rybarczyk, C. Sayrin, S. Gleyzes, J. M. Raimond, M. Brune, and S. Haroche, *Phys. Rev. Lett.* **108**, 243602 (2012).
- [26] J. M. Geremia, *Phys. Rev. Lett.* **97**, 073601 (2006).
- [27] H. Wang, M. Hofheinz, M. Ansmann, R. C. Bialczak, E. Lucero, M. Neeley, A. D. O'Connell, D. Sank, J. Wenner, A. N. Cleland, and J. M. Martinis, *Phys. Rev. Lett.* **101**, 240401 (2008).
- [28] M. Hofheinz, E. Weig, M. Ansmann, R. C. Bialczak, E. Lucero, M. Neeley, A. O'Connell, H. Wang, J. M. Martinis, and A. Cleland, *Nature (London)* **454**, 310 (2008).
- [29] S. Haroche, *Rev. Mod. Phys.* **85**, 1083 (2013).

- [30] P. Campagne-Ibarcq, A. Eickbusch, S. Touzard, E. Zalys-Geller, N. Frattini, V. Sivak, P. Reinhold, S. Puri, S. Shankar, R. Schoelkopf, L. Frunzio, M. Mirrahimi, and M. Devoret, [arXiv:1907.12487](https://arxiv.org/abs/1907.12487).
- [31] M. Kjaergaard, M. E. Schwartz, J. Braumler, P. Krantz, J. I.-J. Wang, S. Gustavsson, and W. D. Oliver, *Annu. Rev. Condens. Matter Phys.* **11**, 369 (2020).
- [32] A. Landig, J. Koski, P. Scarlino, C. Müller, J. Abadillo-Uriel, B. Kratochwil, C. Reichl, W. Wegscheider, S. Coppersmith, M. Friesen, A. Wallraff, T. Ihn, and K. Ensslin, *Nat. Commun.* **10**, 5037 (2019).
- [33] E. T. Jaynes and F. W. Cummings, *Proc. IEEE* **51**, 89 (1963).
- [34] J. Gea-Banacloche, *Phys. Rev. Lett.* **65**, 3385 (1990).
- [35] J. Gea-Banacloche, *Phys. Rev. A* **44**, 5913 (1991).
- [36] J. C. Retamal, C. Saavedra, A. B. Klimov, and S. M. Chumakov, *Phys. Rev. A* **55**, 2413 (1997).
- [37] C. Hermann-Avigliano, N. Cisternas, M. Brune, J.-M. Raimond, and C. Saavedra, *Phys. Rev. A* **91**, 013815 (2015).
- [38] See the Supplemental Material at <http://link.aps.org/supplemental/10.1103/PhysRevLett.125.093603> for a video of the full dynamic of the Wigner function of the intracavity field, an analytical approach to the decoherence-free single atom problem, an analysis of the purity of the final state, and a study of the field dynamics in the Fock states basis, among other details.
- [39] F. A. M. de Oliveira, M. S. Kim, P. L. Knight, and V. Buek, *Phys. Rev. A* **41**, 2645 (1990).
- [40] R. Jozsa, *J. Mod. Opt.* **41**, 2315 (1994).
- [41] A. Gilchrist, N. K. Langford, and M. A. Nielsen, *Phys. Rev. A* **71**, 062310 (2005).
- [42] C. Sayrin, Département de Physique de l'École Normale Supérieure, Laboratoire Kastler Brossel, Ph.D. Thesis, 2011, <https://tel.archives-ouvertes.fr/tel-00654082>.
- [43] M. Penasa, S. Gerlich, T. Rybarczyk, V. Métilon, M. Brune, J. M. Raimond, S. Haroche, L. Davidovich, and I. Dotsenko, *Phys. Rev. A* **94**, 022313 (2016).
- [44] C. Guerlin, J. Bernu, S. Deleglise, C. Sayrin, S. Gleyzes, S. Kuhr, M. Brune, J.-M. Raimond, and S. Haroche, *Nature (London)* **448**, 889 (2007).
- [45] F. Assemat, D. Grosso, A. Signoles, A. Facon, I. Dotsenko, S. Haroche, J. M. Raimond, M. Brune, and S. Gleyzes, *Phys. Rev. Lett.* **123**, 143605 (2019).
- [46] F. Albarelli, A. Ferraro, M. Paternostro, and M. G. A. Paris, *Phys. Rev. A* **93**, 032112 (2016).
- [47] R. J. Lewis-Swan, D. Barberena, J. A. Muniz, J. R. K. Cline, D. Young, J. K. Thompson, and A. M. Rey, *Phys. Rev. Lett.* **124**, 193602 (2020).